HUMAN EVOLUTION

Climate shifts orchestrated hominin interbreeding events across Eurasia

Jiaoyang Ruan[1,2]*, Axel Timmermann[1,2]*, Pasquale Raia[3], Kyung-Sook Yun[1,2], Elke Zeller[1,4], Alessandro Mondanaro[5], Mirko Di Febbraro[6], Danielle Lemmon[1,2], Silvia Castiglione[3], Marina Melchionna[3]

When, where, and how often hominin interbreeding happened is largely unknown. We study the potential for Neanderthal-Denisovan admixture using species distribution models that integrate extensive fossil, archaeological, and genetic data with transient coupled general circulation model simulations of global climate and biomes. Our Pleistocene hindcast of past hominins' habitat suitability reveals pronounced climate-driven zonal shifts in the main overlap region of Denisovans and Neanderthals in central Eurasia. These shifts, which influenced the timing and intensity of potential interbreeding events, can be attributed to the response of climate and vegetation to past variations in atmospheric carbon dioxide and Northern Hemisphere ice-sheet volume. Therefore, glacial-interglacial climate swings likely played an important role in favoring gene flow between archaic humans.

Genomic studies of living and fossil individuals revealed a complex history of interbreeding between *Homo sapiens*—our direct ancestors—and their ancient relatives (*1–7*). As a result, non-Africans today carry ~2% of *Homo neanderthalensis* (Neanderthal) DNA, whereas people from Southeast Asia and Oceania share as much as 2 to 5% of the Denisovan genome (fig. S1) (*7, 8*).

Neanderthals and Denisovans (Fig. 1A) had inhabited and intermittently interbred in Eurasia long before *Homo sapiens* arrived on the continent some 100 thousand years (ka) (*1–3*). Direct evidence for their genetic admixture comes from the discovery of the first-generation (F1) daughter of a Neanderthal mother and a Denisovan father from the Altai mountains ~90 ka (*9*). Further analysis of her father's genome hinted at a deeper-rooted Neanderthal ancestry, which implies a complex history of bidirectional gene flow between the two hominin groups. Recent work (*10*) revealed interbreeding events that date back to ~200 ka. Apart from these genetically reconstructed encounters in Siberia (*9–11*), little is known about where and how frequently Neanderthals and Denisovans interbred throughout their shared history (~400 to 30 ka).

For over a century now, Neanderthal fossils and associated archaeological artifacts have

[1]Center for Climate Physics, Institute for Basic Science, Busan, South Korea. [2]Center for Climate Physics, Pusan National University, Busan, South Korea. [3]DiSTAR, Monte Sant'Angelo, Napoli Università di Napoli Federico II, Naples, Italy. [4]Department of Climate System, Pusan National University, Busan, South Korea. [5]DST, Università degli Studi di Firenze, Florence, Italy. [6]Department of Biosciences and Territory, University of Molise, C. da Fonte Lappone, Pesche, Italy.
*Corresponding author. Email: jiaoyangruan@pusan.ac.kr (J.R.); axel@ibsclimate.org (A.T.)

Fig. 1. Neanderthal and Denisovan locations and their corresponding climate and biome conditions. (**A**) Hominin fossil, archaeological, and genetic data compiled for HSMs; candidate Denisovans (dashed circle). (**B**) Annual mean temperature, precipitation, and NPP extracted for hominin locations and respective age distributions. (**C**) Age-weighted probability of hominin presence in 11 megabiomes.
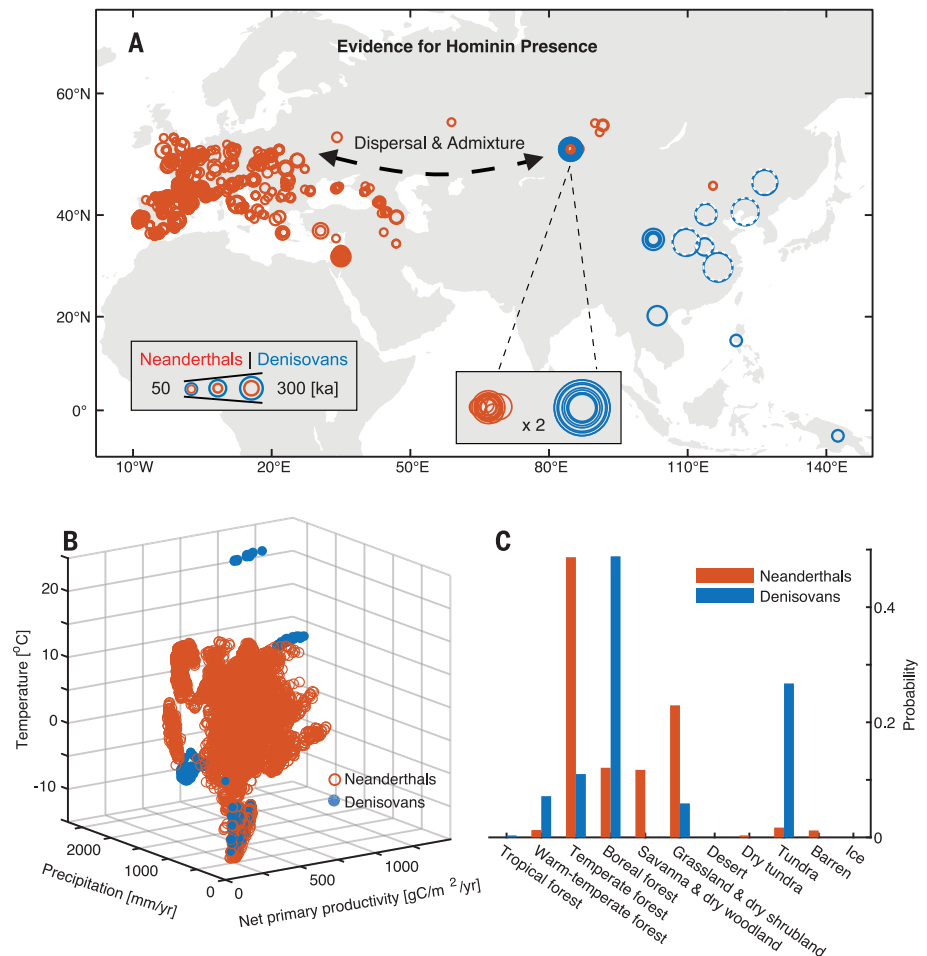
been excavated in Europe, western Asia, and southern Siberia (Fig. 1A) (*12, 13*), which provided fundamental information about their geographical range, climatic preference, behavior, diet, and genetic diversity. By contrast, the fossil remains attributed to Denisovans have been only recovered from the Altai mountains, the Tibetan Plateau, and the northern Annamite Range (*3, 14–16*), with further potential fossil candidates proposed in East Asia (Fig. 1A) (*17*). Genetic analysis further reveals the existence of three deeply divergent Denisovan sublineages, two of which occur in East Asia, that contribute to the present-day human genome pool (*5, 18*). This scattered evidence suggests that Denisovans likely occupied regions characterized by widely different climate and vegetation conditions (fig. S2). The warm and humid conditions of the Southeast Asia monsoon region may have further limited the preservation potential (*19, 20*), which led to the current paucity of fossil remains there. Unfortunately, this scarcity of fossil remains has made it difficult to draw further conclusions regarding their spatiotemporal distribution and possible encounters with other archaic hominins.

Neanderthal and Denisovan habitats

To address these questions, we compiled Denisovan occurrences in space and time (*n* = 22) (data S1) and used a similar compilation prepared for Neanderthals (*n* = 773) drawn from our recent studies (*21, 22*). In these compilations, the same site can have multiple hominin occurrence ages, which are treated as individual samples. By using these hominin presence data and paleoclimate and biome simulations, we built two species distribution models (SDMs)—i.e., a habitat suitability model (HSM) and an environmental niche factor analysis model with phylogenetic imputation (ENphylo), which is specifically designed to give reliable habitat suitability estimates under low number of occurrences (*23, 24*). These models help determine how environmental preferences for the two hominin groups have changed in space and time (fig. S3). Climatic data for the past 400,000 years (CLIM400ka) were extracted from a transient Pleistocene climate simulation conducted with the Community Earth System Model, version 1.2 (*22*). CLIM400ka captures late Pleistocene orbital-scale climate variations in good agreement with various paleo temperature and hydroclimate reconstructions (figs. S4 and S5). Ecological variables used in the SDM, which include net primary productivity (NPP), leaf area index, and megabiome types, were derived from our CLIM400ka-forced version of the BIOME4 simulation (*23, 25*).

Because Denisovans have no formal morphological definition, the identity of the remains that can be ascribed to this hominin
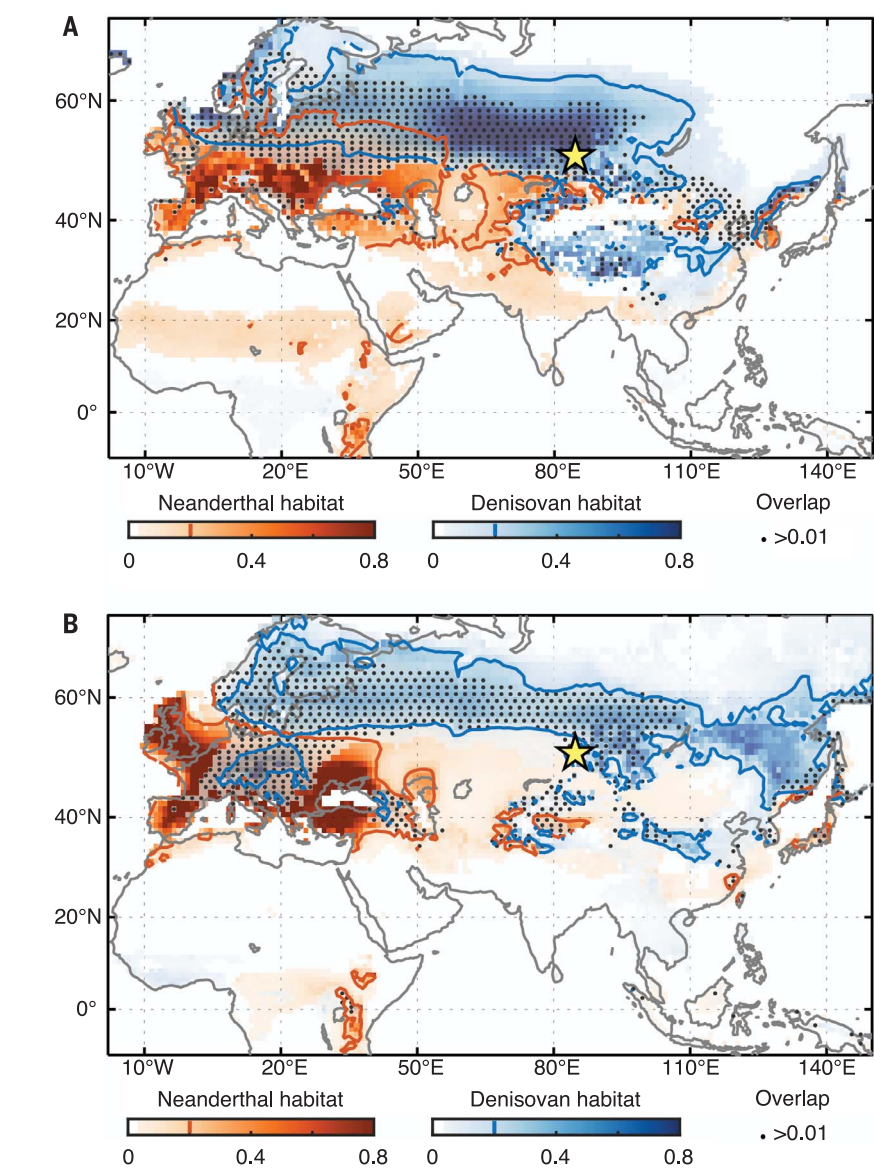

Fig. 2. Neanderthal-Denisovan habitat overlap. (**A** and **B**) Averaged 400- to 30-ka habitats (shading) and overlap (dots) from Mahalanobis HSM (A) and ENphylo- and ecological niche factor analysis (ENFA)–based SDMs (B). The yellow star indicates Denisova cave.

lineage is disputed and mostly based on genetic evidence and scanty fossil remains. Therefore, we generated three different versions of Denisovan datasets (data S1) (*23*), with increasing confidence levels regarding the recognition of possible Denisovan presence. They include an extremely conservative, a conservative, and an extended, more liberal compilation (*23*). The main results of our analyses presented here (Figs. 1 to 4) are obtained for the conservative dataset, and sensitivity experiments with the other data are shown in the supplementary materials. By comparing the corresponding species distribution predictions generated with the three datasets, we gain very similar insights while addressing in part the

effect of potential preservation biases (*19, 20*), which are presumably very pronounced in the Asian monsoon region.

Both Neanderthals and Denisovans are simulated to have lived primarily in environments characterized by annual temperature, precipitation, and NPP of ~−10° to 20°C, ~500 to 1300 mm/year, and ~200 to 800 g of carbon per square meter per year, respectively (Fig. 1B). Yet, compared to Neanderthals, Denisovans were present in hot and humid climates, which points to a comparatively wider niche space. Whereas Neanderthals were more abundant in temperate forests, Denisovans were present in both boreal forest and tundra (Fig. 1C). Fisher's exact test applied to the megabiome
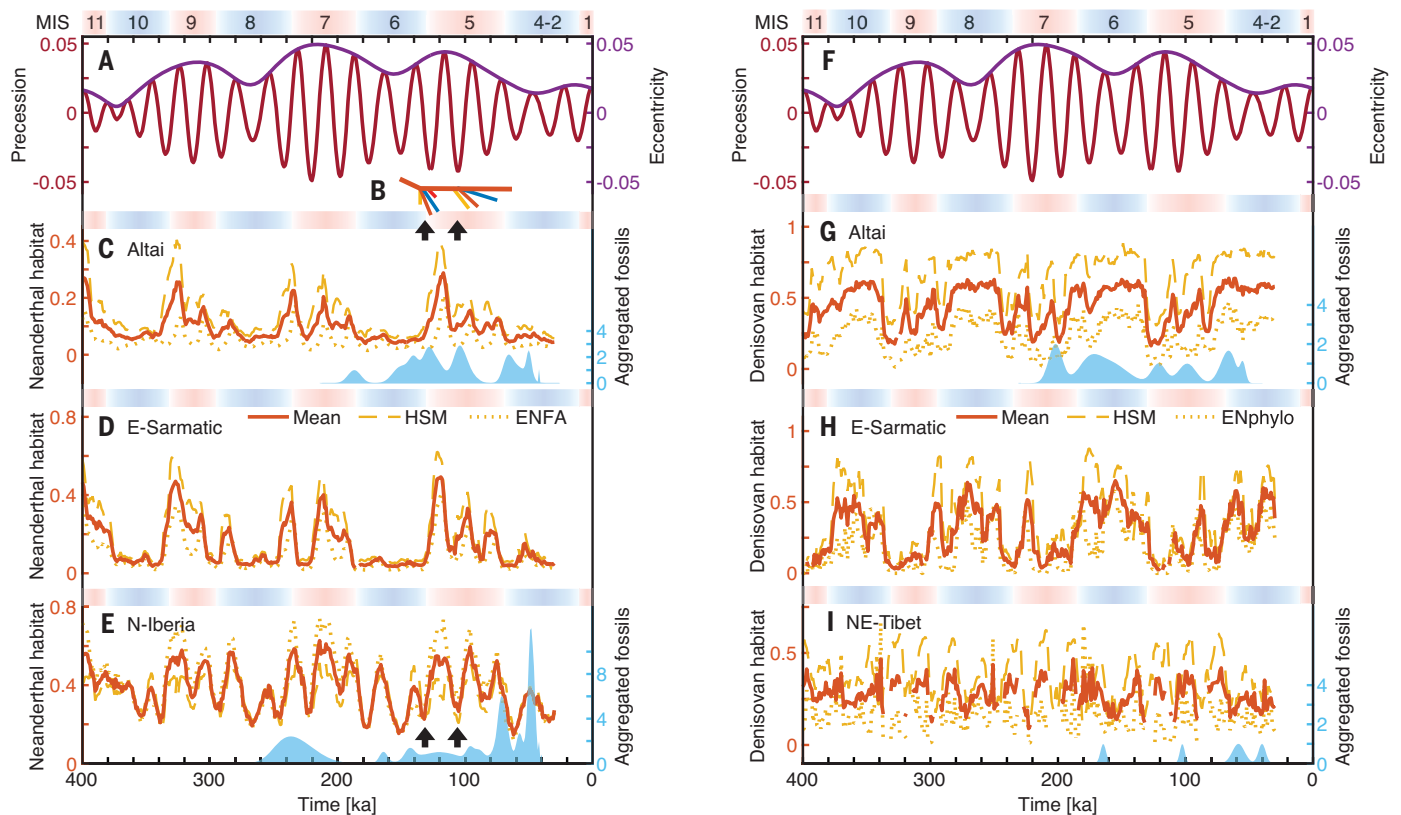
Fig. 3. Temporal evolution of Neanderthal-Denisovan habitat suitability. (**A** to **F**) Eccentricity and precession index. (B) Phylogenetically inferred Neanderthal population turnover events at ~135 ka and ~105 ka (*28*). (C to E) Neanderthal habitat suitability averaged over two SDMs compared with regionally aggregated (3° × 6°) fossil evidence at three selected locations. (**G** to **I**) Same as (C) to (E), but for Denisovans.

preferences (Fig. 1C) of Neanderthals and Denisovans, as well as a Kolmogorov-Smirnov test applied to the three-dimensional climate niche space of both species (Fig. 1B), reveals statistically different distributions ($P < 0.001$), which suggests that the two hominins interacted only where and when their environmental preferences overlapped (Fig. 1A and Fig. 2).

The 400 ka–averaged habitat maps from both SDMs (Fig. 2) document suitable environments for Neanderthals in Europe, consistent with fossil evidence (Fig. 1A), and some fragmented and low-probability regions occurring in western and far eastern Asia and in eastern Africa. Comparatively, Denisovan habitats were geographically more diverse and map to the present-day Eurasian Steppe extending from the Sarmatic Plain to the Mongolian Plateau, parts of Scandinavia, and some pockets in central-eastern Asia. Notably, ENphylo and some fossil input sensitivity experiments simulate suitable Denisovan habitats in central Europe and parts of northeastern Asia (Fig. 2 and fig. S7). Although Denisovan fossils have not been identified with certainty in these regions, the skulls found at Jinniushan, Harbin, and Hualongdong in northeastern China were proposed to be pos-

sible Denisovans (Fig. 1) (*17*, *26*). Uncertainties in Denisovan habitat suitability in Europe as simulated by the SDMs (Fig. 2) may be due to the different choice of climate and vegetation input variables (table S1) (*23*) or because the HSM may be less optimized to handle small sample sizes as compared to ENphylo. Overall, our multimodel simulations of elongated and relatively fragmented Denisovan habitats are qualitatively consistent with the complex admixture patterns of multiple Denisovan sublineages in present-day people (*5*, *18*).

The two hominin habitats show large spatiotemporal variations in response to orbital-scale climate and vegetation shifts (Fig. 3; figs. S7, S8, and S10 to S14; and movies S1 and S2). Empirical orthogonal function (EOF) analysis (*27*) of Eurasian Neanderthal habitats reveals that the first two leading EOF modes, which explain ~63% of the total variance, are dominated by climate variability associated with the eccentricity, CO_2 (80– to 120–thousand year periodicity) and precession forcings (19– to 23–thousand year periodicity) (fig. S12), respectively. In three selected regions of anthropological interest (i.e., the Altai, Sarmatic Plain, and Iberia), high habitat suitability consistently occurs during periods of elevated eccentricity and precession (Fig. 3, C to E). At the

Altai, these periods coincide with warmer and wetter climates suggested by both our model simulation and regional proxy data (figs. S4, S5, and S13). Notably, the widespread lower habitability at two precession minima in the marine isotope stage (MIS) 5 corresponds well with the phylogenetically inferred Neanderthal turnover events in Europe at ~135 ka and ~105 ka (Fig. 3B) (*28*). Neanderthal habitats expand in central and northeastern Europe and southern Siberia (fig. S10A), with a ~69% increase in habitable area (at suitability >0.2) during the past four interglacial periods relative to glacial periods. Conversely, glacial Neanderthal habitats are concentrated in southern Europe and north to the Black Sea (fig. S10B), as documented by the moderate habitability in northern Iberia throughout glacial cycles (Fig. 3E). These regions coincide with the previously reported glacial refugia of various fauna (*29*) and Neanderthals (*30*). The spatially diverse responses of glacial-interglacial habitats may have been one of the reasons for past hominin migrations inside Europe and a candidate hypothesis to explain Neanderthal haplogroup separations (*31*).

The principal components of the first two leading EOF modes of Eurasian Denisovan habitats, which explain ~60% of the total variance,
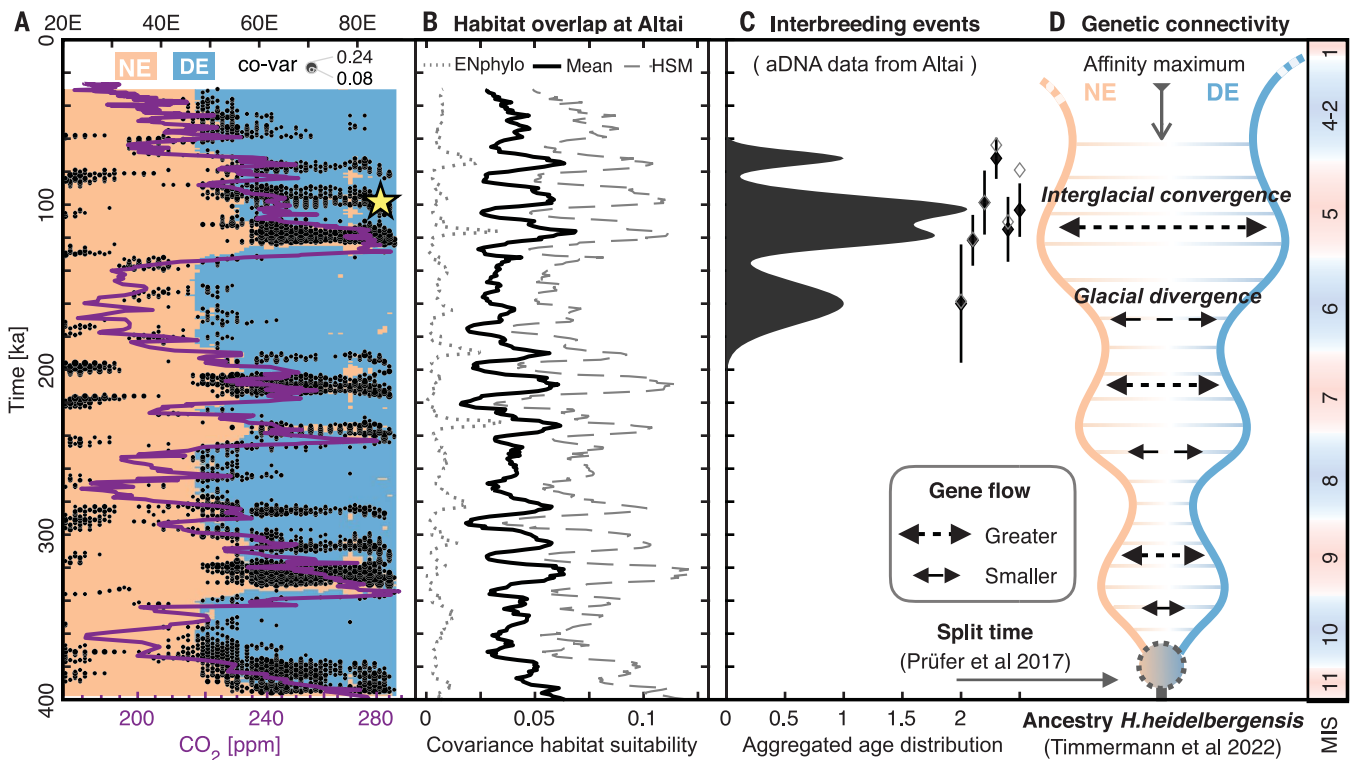
Fig. 4. Spatiotemporal habitat overlap and genetic Denisovan-Neanderthal connectivity. (**A**) Time-longitude diagram of HSM-simulated Neanderthal-Denisovan habitats (shading at suitability >0.2) and overlap (dots); atmospheric CO_2 content (magenta line). Inserted star indicates Denisova cave ~90-thousand-year-old F1 hybrid. co-var, covariability between Denisovan and Neanderthal habitats; DE, preferred Denisovan habitat; NE, preferred Neander-thal habitat; ppm, parts per million. (**B**) Altai habitat overlap probability averaged over 3° × 6° box encompassing Denisova cave. (**C**) Interbreeding chronology of two populations derived from the Altai fossil genomes with aggregated age probability distribution of six identified interbreeding events (shading). aDNA, ancient DNA. (**D**) Schematic of climate effects on genetic Neanderthal-Denisovan connectivity after hypothesized split from common ancestry ~400 ka (*1, 22*).

show similar orbital-scale variability as for Neanderthals (fig. S14). There is a small expansion (~10%) in habitable areas (at suitability >0.2) during interglacial periods. Responding to glacial cooling, Denisovan habitats vanish in Scandinavia, mildly increase in its core areas from eastern Europe to Siberia, and show massive fragmentation in Asia (fig. S11). Unlike Neanderthals in the Altai and the Sarmatic Plain, optimal Denisovan habitats appear under low eccentricity yet high precession (boreal summer insolation minimum) conditions (Fig. 3, G and H), whereas opposing behaviors occur in the Northeast Tibetan Plateau (Fig. 3I). These spatiotemporal Denisovan habitat patterns were repeatedly observed in the Denisovan data sensitivity simulations with both extended and extremely conservative compilations (figs. S7 and S8).

Habitat overlap as a proxy for interbreeding

To determine where and when Neanderthals and Denisovans potentially interbred, we computed the covariance (or overlap) of their respective habitat suitability over time (*23*). The 400-ka habitat overlaps from both SDMs reveal contact hotspots in central Eurasia, the

Caucasus, and the Tianshan and Changbai mountain ranges (Fig. 2, dotted areas). The first region, which encloses the Altai as its eastern end, is consistent with the presence of an F1 hybrid (*9*). A closer examination of this hybridization zone reveals temporal shifts in an east-west direction that occur in unison with the glacial-interglacial climate variability over the past 400 ka (Fig. 4 and fig. S15). For instance, Denisovans and Neanderthals exhibited high contact probability in the Siberian Altai, mostly during interglacial periods MIS 5, 7, and 9. There is also a close match between this zonal seesaw pattern of Denisovan and Neanderthal contact and the long-term change in atmospheric carbon dioxide concentration (Fig. 4A) (*32*). We find that the elevated CO_2 and mild interglacial climate promote the temperate forest to extend across central Eurasia (fig. S16A), which facilitates the northeastward dispersal of Neanderthals (fig. S10A) (*12*) and leads to a territorial encroachment with preexisting Altai Denisovans. By contrast, the lower CO_2 and corresponding harsher glacial climate jointly push the boreal forest range equatorward in central Eurasia (fig. S16B), which may facili-

tate the backflow of Denisovans into Europe (fig. S11B). This analysis suggests that greenhouse gases played a pivotal role in regulating past population dispersal and admixture across Eurasia, through their direct influences on surface temperature and overall moisture availability and because of the simulated CO_2 fertilization effect on vegetation (*33*). Nevertheless, the relative contribution to vegetation shifts on Milanković scales may vary regionally; a recent study pointed to a more complex interplay of climate, CO_2, and other environmental factors in determining vegetation covers such as in tropical Africa (*34*). To further document the role of extratropical temperatures in orchestrating the Neanderthal-Denisovan admixture dynamics, we conducted additional sensitivity experiments (*23*), in which we artificially scaled the amplitude of global temperature variations on Milanković timescales by 0, 70, and 130%. The results (fig. S17) show that CO_2-driven extratropical temperature fluctuations are necessary to obtain the 80- to 120-thousand year variability in hominin overlap. Calculations for a 70 and 130% temperature scaling further reveal similar EOF patterns in habitat overlap variability compared with the

original simulation (fig. S12), which thereby demonstrates the robustness of our results regarding uncertainties in the simulated temperature evolution.

Paleogenomic implications

We further compared our simulation of hominin overlap with a recent synthesis study of fossil genomes from the Altai regions, which had identified at least six episodes of interbreeding between Denisovans and Neanderthals (*10*). To facilitate this comparison, we calculated the absolute times of these episodes by adding the fossil dates from original publications to the molecular clock–based relative mixture time estimates (data S2) and accounting for dating error propagation. The results show that among these six episodes (*10*), the five younger events cluster during the warm MIS 5, whereas the oldest event, although with considerable dating uncertainty, occurs in the cooler MIS 6 (Fig. 4C). Because some of these events occurred thousands of years earlier than the fossil dates, they could have happened in places far away from the places where the specimens were found. Our simulation of Neanderthal-Denisovan overlap suggests that these MIS 5 interbreeding events took place in central-southern Siberia (Fig. 4, A and B), which is consistent with the finding of the F1 hybrid fossil (*9*). By contrast, the MIS 6 event likely happened in eastern Europe.

Whereas bidirectional gene flow between Denisovans and Neanderthals occurred in Siberia, the few European Neanderthal genomes have shown little evidence for admixtures with the Altai Denisovans (*10*). Nevertheless, large-sample genetic analyses have recently revealed Denisovan ancestry in modern European populations in France (*35*) and in Iceland (*36*), which suggests the possibility for more widespread and prevalent interbreeding than previously thought. These results are consistent with our model simulations, which indicate the presence of suitable Denisovan habitats in Europe under optimal orbital conditions (Figs. 2 and 4 and figs. S7, S8, and S14).

Although Denisovans and Neanderthals went through distinct population histories since their split from common ancestry (*2*, *3*), we argue that they were not subject to any reproductive isolation during past glacial cycles (*9*, *10*). In line with previous findings, our analyses support the notion of long-term connectivity between the two hominins and document an admixture hotspot region in central Eurasia (Fig. 2). Moreover, our study reveals that orbitally driven changes in regional climate and vegetation shifted this hybrid zone in an east-west direction with interglacial conditions favoring an eastward intensification and genetic convergence, whereas glacial conditions were associated with occasional interbreeding events in Europe. Our results further demonstrate that climate-driven variations in paired hominin habitats can explain the interbreeding dynamics of Neanderthals and Denisovans during the late Pleistocene and the corresponding flow of genes (Fig. 4). These climate-mediated events have played an essential role in shaping the genomic ancestry of modern humans, which leaves an important legacy even in our present-day population.

REFERENCES AND NOTES

1. K. Prüfer *et al.*, *Science* **358**, 655–658 (2017).
2. K. Prüfer *et al.*, *Nature* **505**, 43–49 (2014).
3. D. Reich *et al.*, *Nature* **468**, 1053–1060 (2010).
4. D. Reich *et al.*, *Am. J. Hum. Genet.* **89**, 516–528 (2011).
5. G. S. Jacobs *et al.*, *Cell* **177**, 1010–1021.e32 (2019).
6. R. E. Green *et al.*, *Science* **328**, 710–722 (2010).
7. M. Larena *et al.*, *Curr. Biol.* **31**, 4219–4230.e10 (2021).
8. S. Sankararaman, S. Mallick, N. Patterson, D. Reich, *Curr. Biol.* **26**, 1241–1247 (2016).
9. V. Slon *et al.*, *Nature* **561**, 113–116 (2018).
10. B. M. Peter, bioRxiv 2020.03.13.990523 [Preprint] (2020).
11. Z. Jacobs *et al.*, *Nature* **565**, 594–599 (2019).
12. K. A. Kolobova *et al.*, *Proc. Natl. Acad. Sci. U.S.A.* **117**, 2879–2885 (2020).
13. W. Roebroeks, M. Soressi, *Proc. Natl. Acad. Sci. U.S.A.* **113**, 6372–6379 (2016).
14. F. Chen *et al.*, *Nature* **569**, 409–412 (2019).
15. F. Demeter *et al.*, *Nat. Commun.* **13**, 2557 (2022).
16. D. Zhang *et al.*, *Science* **370**, 584–587 (2020).
17. A. Bergström, C. Stringer, M. Hajdinjak, E. M. L. Scerri, P. Skoglund, *Nature* **590**, 229–237 (2021).
18. S. R. Browning, B. L. Browning, Y. Zhou, S. Tucci, J. M. Akey, *Cell* **173**, 53–61.e9 (2018).
19. E. Cornelissen, in *Africa from MIS 6-2: Population Dynamics and Paleoenvironments*, S. C. Jones, B. A. Stewart, Eds. (Springer, 2016), pp. 301–319.
20. C. Padilla-Iglesias *et al.*, *Proc. Natl. Acad. Sci. U.S.A.* **119**, e2113936119 (2022).
21. P. Raia *et al.*, *One Earth* **3**, 480–490 (2020).
22. A. Timmermann *et al.*, *Nature* **604**, 495–501 (2022).
23. Materials and methods are available as supplementary materials.
24. A. Mondanaro *et al.*, *Methods Ecol. Evol.* **14**, 911–922 (2023).
25. E. Zeller *et al.*, *Science* **380**, 604–608 (2023).
26. A. Gibbons, *Science* **355**, 899 (2017).
27. A. Hannachi, I. T. Jolliffe, D. B. Stephenson, *Int. J. Climatol.* **27**, 1119–1152 (2007).
28. B. Vernot *et al.*, *Science* **372**, eabf1667 (2021).
29. G. Hewitt, *Nature* **405**, 907–913 (2000).
30. M. Melchionna *et al.*, *Palaeogeogr. Palaeoclimatol. Palaeoecol.* **496**, 146–154 (2018).
31. V. Fabre, S. Condemi, A. Degioanni, *PLOS ONE* **4**, e5151 (2009).
32. B. Bereiter *et al.*, *Geophys. Res. Lett.* **42**, 542–549 (2015).
33. W. Chen *et al.*, *Quat. Sci. Rev.* **218**, 293–305 (2019).
34. W. D. Gosling *et al.*, *Science* **376**, 653–656 (2022).
35. A. Bergström *et al.*, *Science* **367**, eaay5012 (2020).
36. L. Skov *et al.*, *Nature* **582**, 78–83 (2020).
37. J. Ruan *et al.*, Neanderthal and Denisovan Habitat Simulation, ICCP Dataserver (2023).
38. J. Ruan *et al.*, Ruan et al 2023 Science, ICCP Dataserver (2023).

SUPPLEMENTARY MATERIALS

science.org/doi/10.1126/science.add4459
Materials and Methods
Figs. S1 to S17
Table S1
References (*39–84*)
MDAR Reproducibility Checklist
Movies S1 and S2
Data S1 and S2

Climate shifts orchestrated hominin interbreeding events across Eurasia

Jiaoyang Ruan, Axel Timmermann, Pasquale Raia, Kyung-Sook Yun, Elke Zeller, Alessandro Mondanaro, Mirko Di Febbraro, Danielle Lemmon, Silvia Castiglione, and Marina Melchionna

Editor's summary

Most of what we know about hominin evolution comes from fossil evidence, and these fossils come from a world shaped by climate and ecological dynamics, as ours is today. The ability to estimate these past environments permits us to better understand the forces that shaped our evolution. Using climate models to estimate past environments and spatial distribution models to predict species occurrence, two studies now reveal details about hominin evolution that fossils alone cannot (see the Perspective by Beverly). Looking at habitat overlap for Neanderthals and Denisovans, Ruan *et al.* found patterns of interbreeding between the two that correlate with climate and environmental change in Eurasia. Margari *et al.* have identified a previously unknown climate-driven depopulation of hominins in southern Europe during the early Pleistocene. —Sacha Vignieri

View the article online
https://www.science.org/doi/10.1126/science.add4459
Permissions
https://www.science.org/help/reprints-and-permissions

Use of this article is subject to the Terms of service